Systematic behavior of one- and two-nucleon transfer reactions induced by medium-weight projectiles

K. E. Rehm, C. Beck,* A. van den Berg,† D. G. Kovar, L. L. Lee,‡ W. C. Ma,§
F. Videbaek, and T. F. Wang**
Argonne National Laboratory, Physics Division, Argonne, Illinois 60439
(Received 27 December 1989)

Few-nucleon transfer reactions have been measured for the systems $^{64}Ni+^{208}Pb$ and $^{80}Se+^{208}Pb$ at energies slightly above the Coulomb barrier. Together with previous data, heavy-ion-induced transfer reactions on ^{208}Pb have now been studied with projectiles in the mass range $A=12-86$. The experimental total reaction cross sections and the yields for quasielastic processes are compared with various theoretical predictions. For the one- and two-nucleon transfer reactions a systematic behavior of the energy- and angle-integrated cross sections is observed. This behavior can be understood within a simple semiclassical model. A comparison of the cross-section ratios between one- and two-neutron and the one- and the two-proton transfer reactions indicates that the two-proton-transfer process shows an enhancement with respect to the one-proton transfer reaction.

I. INTRODUCTION

The magic numbers $N=126$ and $Z=82$ have made ^{208}Pb an ideal target nucleus for nuclear reaction studies. ^{208}Pb has previously been used in a large number of light-ion-induced reactions, but relatively little is known about its interactions with heavier projectiles. Recently, transfer reactions with ^{208}Pb targets and projectiles in the mass range between ^{28}Si and ^{86}Kr have been investigated at energies slightly above the Coulomb barrier[1-4] and it was observed that for these systems quasielastic channels give considerable contributions to the total reaction cross sections. Quasielastic reactions also strongly influence heavy-ion-induced fusion reactions at low bombarding energies. It has been observed in a large number of systems that the experimental fusion probability at energies below the Coulomb barrier is much larger than expected on the basis of one-dimensional barrier penetration calculations.[5,6] This enhancement is generally attributed to channel-coupling effects with inelastic scattering being the strongest channel.[7] In several cases transfer reactions are also found to be of importance.[8] Experimental values for the cross sections of quasielastic channels are available only for a few systems. On the other hand, a knowledge of the transfer strength would be helpful in order to estimate the effect of coupled-channel calculations on the fusion probability. While the strength of inelastic scattering can in most cases be reliably predicted by distorted-wave Born approximation (DWBA) or coupled-channel (CC) calculations,[9] predicting the strength for transfer reactions is more complicated. Reliable calculations of one-particle transfer reactions can usually be performed within the framework of the DWBA. These calculations, however, are often quite time consuming because of the many different channels involved in the calculations. In addition, in general, not all spectroscopic factors are known for the states involved in the transfer process. Two-particle transfer reactions, which in some cases are predicted to be important for the fusion enhancement, are even more difficult to calculate since at low bombarding energies these reactions occur mainly via multistep processes.[10] The purpose of this paper is to investigate if a systematic picture for heavy-ion-induced transfer reactions can be obtained. We have therefore extended our measurements of transfer reactions to the heavier systems $^{64}Ni+^{208}Pb$ and $^{80}Se+^{208}Pb$. Together with previous experiments involving lighter projectiles (^{12}C,^{16}O) (Refs. 11 and 12) the strength of quasielastic transfer reactions can therefore be studied in more detail covering a large range both in projectile mass and in Q value.

II. EXPERIMENTAL DETAILS

The experiments were performed with beams of 380 MeV ^{64}Ni and 525 MeV ^{80}Se, obtained from the Argonne superconducting linac accelerator ATLAS. Typical beam currents were about 1 particle nA. The targets consisted of 200-$\mu g/cm^2$ ^{208}Pb evaporated on 15-$\mu g/cm^2$ C backings. The outgoing particles were momentum analyzed in a split pole spectrograph and detected in the focal plane by a position-sensitive ionization chamber.[13] Details of the data analysis have already been given elsewhere.[14] For ^{64}Ni a complete separation of the outgoing particles with respect to their mass and charge was achieved. For Se particles only mass identification was obtained (see Fig. 1), since the ΔE resolution of the ionization chamber did not allow a separation of the various elements around $Z=34$. While this has no influence on the conclusions for the neutron-pickup reactions, one-nucleon-stripping reactions are affected by this deficiency (see Sec. III). The energy resolution (limited by the energy straggling in the thick ^{208}Pb targets) was about 3 MeV for the ^{64}Ni beam and 4 MeV for the ^{80}Se beam. A separation of individual states was therefore not possible.

III. EXPERIMENTAL RESULTS

Angular distributions for elastic scattering [including inelastic scattering to low-lying states below 3 MeV

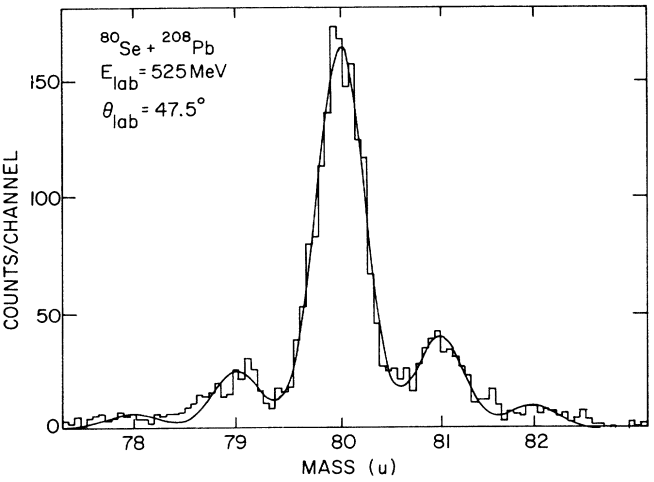

FIG. 1. Mass spectrum as measured with the focal plane detector in the split pole spectrograph for the system ^{80}Se+^{208}Pb at E_{lab}=525 MeV. The full drawn curve is the result of a least-squares fit to the data assuming a Gaussian distribution.

(^{64}Ni) or 4 MeV (^{80}Se) excitation energy] and for energy-integrated one- and two-nucleon transfer reactions are shown in Fig. 2. The solid lines in the angular distributions for "elastic" scattering are the result of coupled-channel calculations with the code PTOLEMY,[15] using potential parameters (V=100 MeV, W=40 MeV, $r_0=r_{i0}$=1.28 fm, and $a=a_i$=0.5 fm for ^{80}Se and V=100 MeV, W=40 MeV, $r_0=r_{i0}$=1.25 fm, a=0.35 fm, and a_i=0.60 fm for ^{64}Ni, respectively). In order to keep the calculations as simple as possible only the coupling to the lowest states in both projectile and target have been taken into account. The $B(EL)$ values used were $B(E2,^{64}\text{Ni})=0.065\ e^2\text{b}^2$,[16] $B(E2,^{80}\text{Se})=0.498\ e^2\text{b}^2$,[17] and $B(E3,^{208}\text{Pb})=0.611\ e^2\text{b}^3$.[18] The dashed lines in Fig. 2 are the calculated angular distributions for pure elastic scattering, which show a gradual falloff from the Rutherford values at the most forward angles. In addition, an increase in the cross section at angles of about 60° can be observed for the ^{80}Se+^{208}Pb reaction. This behavior, which is caused by backfeeding from the strongly excited 2^+ state in ^{80}Se, has already been predicted in Ref. 19. The sum of elastic and inelastic scattering is in reasonable agreement with the measured angular distribution, considering that no least-squares fit has been made.

The angular distributions for one- and two-particle transfer reactions are generally bell shaped with a maximum at an angle which is slightly forward of the quarterpoint angle obtained from the angular distributions for "elastic" scattering. The integrated cross sections for one- and two-particle transfer reactions are summarized in Table I. In both systems the strongest channel is the one-neutron-pickup reaction (^{64}Ni,^{65}Ni) and (^{80}Se,^{81}Se), respectively.

While ^{65}Ni has clearly been identified with respect to its mass and charge for the ^{64}Ni+^{208}Pb system, only the

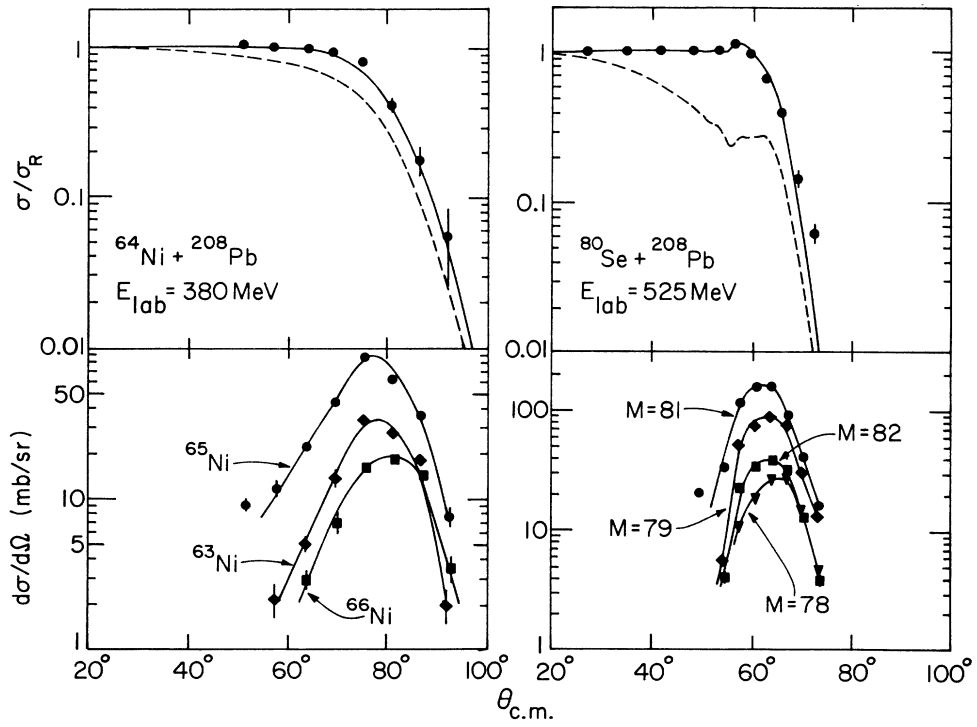

FIG. 2. Top: Angular distributions for elastic scattering including inelastic excitation of low-lying states for the two systems ^{64}Ni+^{208}Pb and ^{80}Se+^{208}Pb. The solid and dashed lines are the results of CC calculations as explained in the text. Bottom: Angular distributions for one- and two-nucleon transfer reactions as measured for ^{64}Ni+^{208}Pb and ^{80}Se+^{208}Pb. The solid lines serve to guide the eye.

TABLE I. Cross sections for one- and two-neutron reactions measured in the systems $^{64}Ni+^{208}Pb$ and $^{80}Se+^{208}Pb$.

Projectile	1-n-pickup $A \rightarrow A+1$ (mb)	2n-pickup $A \rightarrow A+2$ (mb)	1-n-stripping $A \rightarrow A-1$ (mb)
^{64}Ni	160	40	60
^{80}Se[a]	194	47	104

[a]Transfer cross sections measured with ^{80}Se include contributions from both neutron and proton transfer.

mass has been uniquely determined for the system $^{80}Se+^{208}Pb$. Based on the systematics for heavy-ion-induced transfer reactions (Refs. 1–4) and on the more favorable Q matching ($Q_{gg}=-0.667$ MeV) it can be assumed that for the one-nucleon-pickup reaction ($^{80}Se,^{81}Se$) is the dominant reaction mode. The competing ($^{80}Se,^{81}Br$) reaction has a ground-state Q value of $Q_{gg}=-0.512$ MeV, while the optimum Q value is calculated[20] to be +6.1 MeV. The same argument holds for the two-nucleon-pickup reaction, which is very likely dominated by the ($^{80}Se,^{82}Se$) channel.

The situation is less clear for the stripping reactions. In these cases previous studies with lighter projectiles ($^{46,48,50}Ti$) on ^{208}Pb targets[3] have revealed that a large fraction of the one-nucleon-stripping cross section has to be attributed to the one-proton-stripping reaction. This again can be understood by the more favorable matching conditions. Recent data for the system $^{76}Ge+^{186}W$, where a good Z separation was achieved,[21] also show that the cross sections for one-neutron-stripping reactions are considerably smaller than those for one-proton stripping.

As observed in previous studies,[1–4] it is found that these few-nucleon transfer reactions are associated with small energy losses (quasielastic reactions). Processes with more negative Q values are mainly dominated by more complex multiparticle (in particular, charged-particle) transfer reactions. Figure 3 shows the cross sections associated with quasielastic and deep-inelastic reactions as a function of the scattering angle. As discussed in Ref. 3 no clear distinction between the two processes exists. Similar to our previous analyses, processes with $Q>-30$ MeV have been labeled as "quasielastic" and processes with $Q<-30$ MeV as "deep-inelastic" collisions. From the measured angular distributions for "quasielastic" scattering integrated cross sections can be extracted for both systems. For deep-inelastic scattering an integrated cross section can only be quoted for $^{80}Se+^{208}Pb$. For $^{64}Ni+^{208}Pb$ the angular range of the data does not allow for an extrapolation of the cross sections to smaller angles. The cross sections associated with quasielastic and deep-inelastic processes are $\sigma_{qe}(^{64}Ni)=420$ mb, $\sigma_{qe}(^{80}Se)=410$ mb, and $\sigma_{di}(^{80}Se)=1500$ mb. The sum of quasielastic and deep-inelastic cross sections for the $^{80}Se+^{208}Pb$ system is then 1910 ± 150 mb in good agreement with the total reaction cross section of 2045 mb obtained from the CC calculation mentioned above. For the case of $^{64}Ni+^{208}Pb$ one can estimate the deep-inelastic cross section from the total reaction cross section $\sigma(^{64}Ni)=1430$ mb and the measured quasifission contribution[22] $\sigma_{qf}(^{64}Ni)=115$ mb to be $\sigma_{di}(^{64}Ni)=895$ mb.

IV. CROSS-SECTION SYSTEMATICS

A. Total reaction cross sections

Table II summarizes the total reaction cross sections measured for ^{208}Pb targets with various projec-

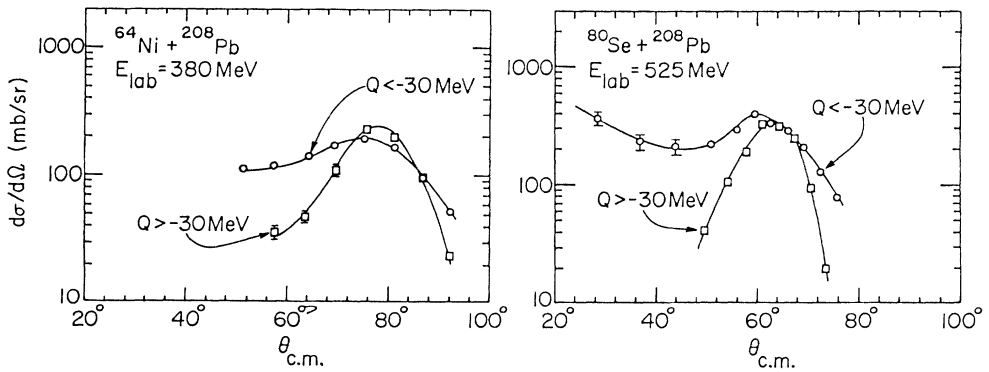

FIG. 3. Angular distributions for quasielastic ($Q>-30$ MeV) and deep-inelastic ($Q<-30$ MeV) processes measured for the two systems $^{64}Ni+^{208}Pb$ and $^{80}Se+^{208}Pb$. The solid lines serve to guide the eye.

TABLE II. Total reaction cross sections for heavy-ion-induced reactions on ^{208}Pb.

Projectile	E_{lab} (MeV)	$\theta_{1/4}$ (deg)	σ_{react} (mb)	Ref.
^{12}C	96.0	56	1806	11
^{16}O	104	78	1160	23
^{28}Si	225	53	2260	8
^{37}Cl	250	65	1830	7
^{48}Ti	300	78.5	1460	9
^{58}Ni	375	82	1450	7
^{64}Ni	380	84.5	1430	This work
^{80}Se	525	68	2050	This work
^{86}Kr	695	46.5	3300	4

tiles.[1-4,11,12] Comparing these values it has to be kept in mind that for the lighter projectiles ($A<48$) inelastic excitations have been separated from elastic scattering and the total reaction cross sections therefore contain contributions from inelastic scattering, transfer, fission, and fusion reactions. For the heavier projectiles ($A\geq 48$) no separation between elastic and inelastic scattering has been achieved and the total reaction cross sections therefore do not contain contributions from inelastic scattering, but are all due to transfer reactions and fusion-fission processes. In order to compare the reaction cross sections which were measured at different energies they were parametrized with the equation

$$\sigma=\pi R^2(1-V/E)\ . \tag{1}$$

The energy above the Coulomb barrier was calculated from the measured quarterpoint angle $\theta_{1/4}$ with the relation

$$\frac{E}{V}=0.5[1+\csc(\theta_{1/4}/2)]\ . \tag{2}$$

The radii for the reaction cross sections extracted for the various systems using Eqs. (1) and (2) are plotted in Fig. 4 as functions of $X=(A_p^{1/3}+A_t^{1/3})$. Also included are the results obtained from the system ^{86}Kr+^{208}Pb (Ref. 4).

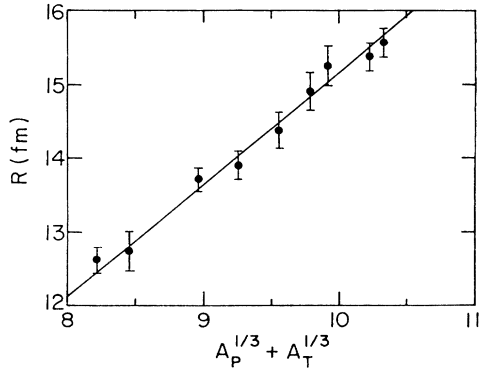

FIG. 4. Interaction radii extracted from the measured total reaction cross sections using Eqs. (1) and (2) plotted vs $A_p^{1/3}+A_t^{1/3}$. The solid line is the result of a linear least-squares fit to the data. See text for details.

The data follow a linear relation as a function of the sum of the two radii for projectile and target over the mass range from $A=12$ to 86. The solid line is the result of a least-squares fit to the data using the relation $R=r_0X$ with a value $r_0=1.519\pm0.009$ fm.

B. Cross sections for deep-inelastic processes

As mentioned in Ref. 3 there is no clear distinction between quasielastic and deep-inelastic reactions. Similar to our previous studies an arbitrary energy cut at $Q=-30$ MeV was chosen for all cases. No data for deep-inelastic reactions are available for the lighter projectiles (^{12}C, ^{16}O, ^{28}Si). Since not very much is known about the energy dependence of the strength for deep-inelastic scattering, only the ratio between the deep-inelastic reaction strength and the total reaction cross sections will be discussed in the following. For the heavier systems this ratio is plotted in Fig. 5 (solid dots). One observes an increase from about 27% obtained for ^{37}Cl to 70% for the heaviest system (^{80}Se) studied so far. Also included in Fig. 5 are the ratios between the fusion-fission cross section (including the quasifission process) and the total reaction cross sections (open squares). They decrease from about 70% for ^{16}O+^{208}Pb (Ref. 23)to 8% for ^{64}Ni+^{208}Pb (Ref. 22). It is interesting to note that the sum of the two contributions which represents a measure of the total reaction strength for close collisions is found to be of the order of 70% at these energies independent of the mass of the projectile. It is only the partition of this strength going either to fusion-fission (for lighter projectiles) or into deep-inelastic scattering that changes with increasing mass of the projectile. It should also be noted that this value of about 70% is strongly energy dependent. It is known[24] that the relative contribution of quasielastic processes to the total reaction strength, which from these measurements is estimated to be around 30%, increases strongly such that quasielastic scattering becomes the dominant reaction mode at lower bombarding energies.

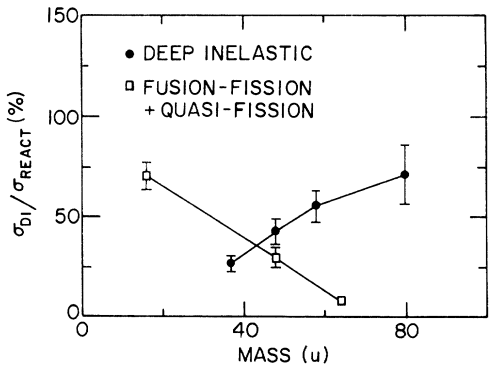

FIG. 5. Ratio of the deep-inelastic ($Q<-30$ MeV) to the total reaction cross section for various systems, plotted versus the mass of the projectile (solid dots). The open squares are the ratio between fission (including quasifission) processes and total reaction cross sections as measured for various systems involving ^{208}Pb targets.

Similar percentages (40% for the quasielastic reactions and 60% for more central collisions) have been previously found for the lighter system $^{58}Ni+^{124}Sn$ (Ref. 24).

C. Quasielastic processes

As seen in Fig. 5 about 30% of the total reaction strength (excluding inelastic scattering) is available for grazing collisions in the reaction systems investigated in this study. This corresponds to cross sections of about 300–500 mb. As was pointed out earlier (Ref. 1) the neutron transfer dominates the quasielastic reactions for heavier projectiles. In Fig. 6 the relative contributions of the quasielastic neutron transfers to the total quasielastic ($Q > -30$ MeV) cross section are plotted as functions of the mass of the projectile. This contribution increases from about 40% for $^{16}O+^{208}Pb$ to about 70% for $^{80}Se+^{208}Pb$ making neutron transfer (in particular, one-neutron transfer channels) the most dominant quasielastic transfer channel for reactions induced by medium-weight projectiles.

Various semiclassical models have been developed to predict the strength of quasielastic reactions. In the model of Frahn[25] quasielastic reactions are associated with an l window of width Δ located around the grazing angular momentum Λ, where Δ is obtained from the falloff of the transmission coefficients from 1 to 0 with increasing l. While in Ref. 25 no comparison with experimental values has been made, a later study[26] in lighter systems found good agreement between theory and experiment. In a more recent model by Brosa *et al.* (Ref. 27) the quasielastic reactions are distinguished from deep-inelastic collisions by a different width of the transfer window between the two colliding nuclei. In Ref. 27 the theory was compared to selected experiments in which the elastic and quasielastic (especially neutron-transfer) channels were not well separated in most cases. In addition to quasielastic cross sections, both models are also able to predict values for the total reaction cross sections. Figure 7 summarizes the results from Ref. 25 (solid lines) and Ref. 27 (dashed lines) together with the experimental values for total reaction and quasielastic cross sections. The values for Δ used in calculating the cross sections in the model of Frahn were interpolated from the numbers given in Ref. 25 or taken from the transmission coefficients in actual optical-model calculations. They are typically between 3 (for ^{16}O) and 4.5 (for ^{80}Se). The radius parameter r_0 was chosen to be 1.44 fm. As can be seen from Fig. 7(a) the total reaction cross sections of Ref. 25 are in very good agreement with the experimental results, while the prediction of Ref. 27, which has no adjustable parameter, underpredicts the cross sections for the heavier systems by 200–300 mb. Neither of the two models works well for the quasielastic cross sections. While the model of Frahn is in reasonable agreement with the data for lighter systems (^{12}C,^{16}O) it underpredicts the cross sections for heavier projectiles by a factor of about 3. Contrary to this behavior the model of Brosa *et al.* predicts too small cross sections for light systems with an increase for heavier projectiles. Most of the experimental values are larger than the theoretical prediction by about a factor of 2. It should be mentioned that changing the borderline between quasielastic and deep-inelastic reactions from $Q = -30$ MeV to -20 MeV does not change the experimental quasielastic cross sections significantly since they are mainly dominated by neutron-transfer cross sections, i.e., processes which have Q values larger than -15 MeV.

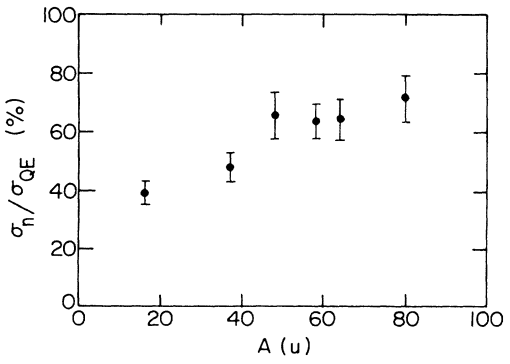

FIG. 6. Relative contribution of neutron-transfer channels to the total quasielastic reaction strength for reactions induced by various projectiles on ^{208}Pb targets.

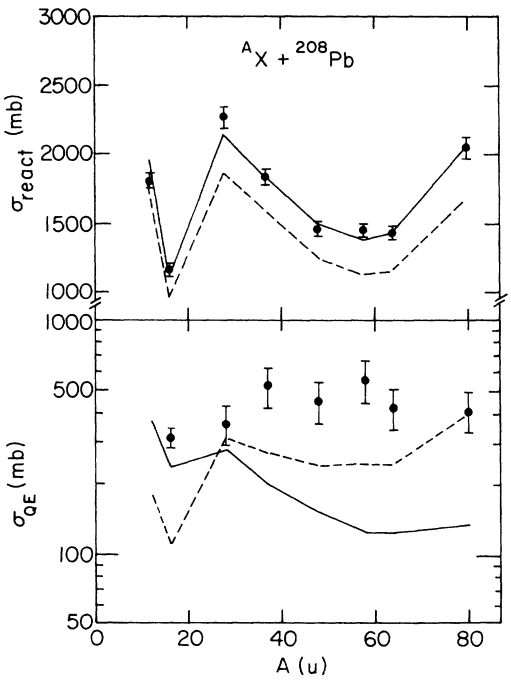

FIG. 7. (a) Total reaction cross sections calculated using equations from Ref. 25 (solid lines) or Ref. 27 (dashed lines) in comparison with experimental values (dots) for systems involving various projectiles on ^{208}Pb targets. (b) Same as (a) but for the quasielastic cross sections.

V. SYSTEMATICS OF NEUTRON-TRANSFER REACTIONS

A. One-neutron transfer

In the following we will discuss to what extent the strength of quasielastic neutron transfers, which are the dominating contributions to quasielastic scattering (see Fig. 6), can be understood within various theoretical models. In Fig. 8 angle- and energy-integrated cross sections for one- and two-neutron transfer reactions induced by projectiles heavier than ^{12}C on ^{208}Pb targets are plotted as functions of the mass number of the projectile (see also Tables III and IV). As can be seen from Fig. 8(a) there is a general increase of the one-neutron-pickup cross sections in going from light (^{12}C) to heavier projectiles (^{58}Ni, ^{80}Se). While the cross section is only 30 mb for the (^{12}C,^{13}C) reaction it increases to about 250 mb for (^{58}Ni,^{59}Ni). But there are also large fluctuations for the strength of these reactions, with neutron-deficient projectiles (^{28}Si,^{58}Ni) usually showing larger pickup cross sections than neutron-rich projectiles (^{64}Ni,^{80}Se). The cross sections for two-neutron-pickup reactions [Fig. 8(b)] seem to follow a similar trend. For the one-neutron-stripping reactions [Fig. 8(c)] even larger fluctuations, as functions of the projectile mass, can be observed.

The strength of neutron-transfer reactions induced by light heavy ions can be reasonably well reproduced by DWBA calculations as shown, e.g., for (^{12}C,^{13}C) (Ref. 11) and (^{16}O,^{17}O) (Ref. 12), where transitions to individual states have been resolved. Even for heavier systems such as ^{58}Ni+^{208}Pb, where individual states could not be resolved, DWBA was able to account for the measured transfer strength quite well.[1,28] For these heavier projectiles, however, the calculations are very complex and time consuming because of the larger number of states involved. While for the lighter systems only about six states in projectile and target have to be taken into account, this number increases to 48 for ^{58}Ni+^{208}Pb. In many cases, in particular for states at high excitation energies, no spectroscopic factors are available to obtain a good estimate for the transfer cross section. It is therefore of interest to investigate whether a simpler method for the determination of energy- and angle-integrated cross sections can be found.

The energy- and angle-integrated cross section can be written as

$$\sigma = \sum_{\substack{i \in \text{projectile} \\ j \in \text{target}}} S_i(\text{projectile}) S_j(\text{target}) \sigma_{ij} \ , \tag{3}$$

where S_i and S_j are the spectroscopic factors for the various single-particle states in projectile and target, respectively, and σ_{ij} is the DWBA cross section involving the states i and j. DWBA calculations with the code PTOLEMY (Ref. 15) have shown that at energies in the vicinity of the Coulomb barrier only the absolute magnitude but not the shape of σ_{ij} depends on the angular momenta of the states involved in the interaction. If many states are involved in the sum in Eq. (3), σ_{ij} can be replaced by an average value $\langle \sigma(\theta) \rangle$ which is independent of i and j. Equation (3) can then be replaced by the approximate equation

$$\sigma = \sum_i S_i(\text{projectile}) \sum_j S_j(\text{target}) \langle \sigma(Q) \rangle \ . \tag{4}$$

The accuracy of this approximation was tested for the systems ^{58}Ni+^{64}Ni and ^{58}Ni+^{208}Pb, by performing DWBA calculations involving 20(^{64}Ni) and 24(^{208}Pb) different spin combinations for projectile and target, respectively. Equations (3) and (4) were found to agree within 15% (^{64}Ni) or 7% (^{208}Pb).

As already outlined briefly in Ref. 29, an important ingredient determining $\langle \sigma(Q) \rangle$ for heavy-ion-induced transfer processes is the ground-state Q value Q_{gg} and the binding energy of the last bound neutron E_n. Q-matching conditions constrain the population to states located in a certain Q window. The shape of this Q window, as obtained from a DWBA calculation for the reaction ^{208}Pb(^{58}Ni,^{59}Ni($\frac{1}{2}^-$))^{207}Pb($\frac{1}{2}^-$) at E_{lab}=375 MeV, is shown in Fig. 9. For neutron transfer this window is located in the vicinity of Q=0 with a width of about 6 MeV. This width is known to increase with increasing bombarding energy. Also shown in Fig. 9 are the various combinations of single-particle states in ^{59}Ni and ^{207}Pb plotted on a Q-value scale for excitation energies below E_x=3.5 MeV. The energy-integrated cross sections for

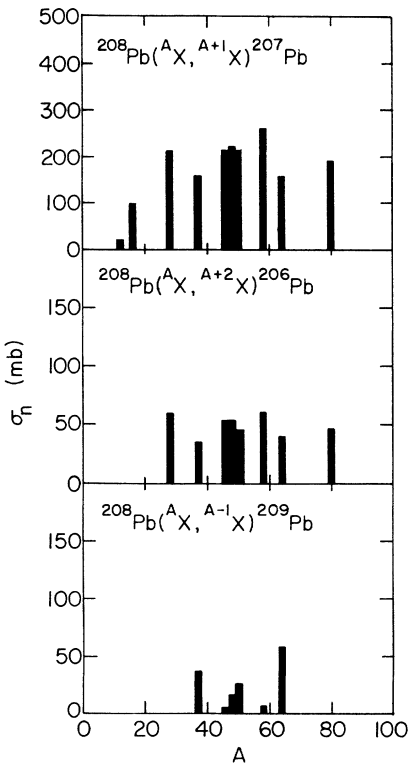

FIG. 8. (a) Energy- and angle-integrated cross sections for one-neutron-pickup cross sections induced by various projectiles on ^{208}Pb targets plotted as a function of the projectile mass. (b) Same as (a) but for two-neutron-pickup reactions. (c) Same as (a) but for one-neutron-stripping reactions.

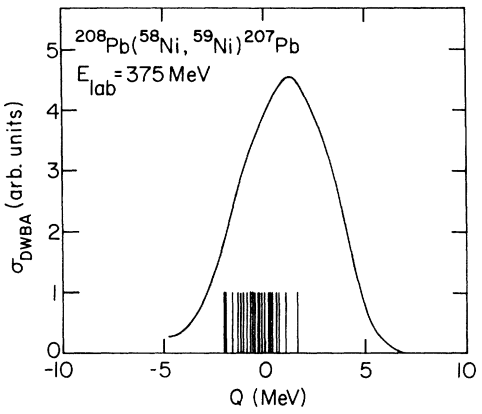

FIG. 9. "Q window" obtained from DWBA calculations for the reaction ^{208}Pb(^{58}Ni,^{59}Ni($\frac{1}{2}^-$))^{207}Pb($\frac{1}{2}^-$). The vertical lines correspond to the various known single-particle states which can be populated in the outgoing nuclei. See text for details.

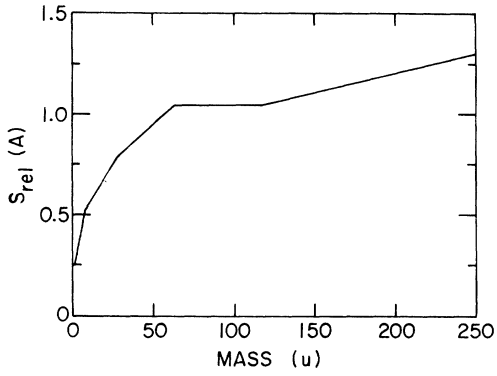

FIG. 10. Number of low-spin ($l \leq 4$) single-particle neutron states as a function of the mass number. The function was normalized to 1 at $A = 58$. See text for details.

neutron-transfer reactions will, in general, be given as the integral

$$\langle \sigma(Q_{gg}) \rangle = \int_{-\infty}^{Q_{gg}} \sigma(Q) dQ \ . \tag{5}$$

Approximating the shape of the Q window with a Gaussian distribution $\sigma \sim \exp(-Q^2/W^2)$ the Q_{gg} dependence of the one-neutron transfer cross sections is given by[29]

$$\langle \sigma(Q_{gg}) \rangle = N \left[1 + \mathrm{erf} \left[\frac{(Q_{gg} - Q_{\mathrm{opt}})}{W} \right] \right] , \tag{6}$$

where N is a normalization constant and W the width of the Q window. Several corrections have to be made to improve the validity of this simple model.

(i) Describing the number of states by a continuum assumes that the level density for single-particle states is large. This is justified for reactions involving even-even projectiles and targets, which lead to even-odd nuclei in the outgoing channel (see Fig. 9). Reactions involving targets with an odd neutron number leading to an even-even residual nucleus with a smaller level density will result in an overprediction of the cross sections. This was shown to be the case for the ^{149}Sm(^{58}Ni,^{59}Ni)^{148}Sm reaction (Ref. 29).

(ii) As already mentioned in Ref. 29, transfer cross sections involving weakly bound neutrons are generally larger than those involving larger binding energies. To compensate for this effect the transfer cross sections are multiplied by a factor $(B_i B_f)^{1.1}$, where the exponent was determined from DWBA calculations. It is these binding-energy-corrected ("reduced") cross sections which are then described by Eq. (6).

(iii) The level density for low-spin ($l < 4$) single-particle states, which carry the largest weight for the one-neutron transfer reactions at low bombarding energies, varies as a function of the mass of the nucleus. For the (^{16}O,^{17}O) reaction only the $s_{1/2}$ and the $d_{5/2}$ states in the projectile contribute to the cross section while for the (^{80}Se,^{81}Se) case four states ($p_{1/2}$, $g_{9/2}$, $p_{3/2}$, and $f_{5/2}$) have to be considered. The number of terms in the sums of the spectroscopic factors in Eq. (4) will therefore depend on the mass of projectile and target, respectively. This correction is especially important when cross sections for projectiles with different masses are compared. The sum of the spectroscopic factors for the projectile $S_p(A)$ is plotted as a function of the mass number in Fig. 10. Since the parameters for Eq. (6) were obtained from a least-squares fit to data involving mainly ^{58}Ni beams it was normalized to be 1 at $A = 58$. A similar curve describes the single-particle level density for the target $S_T(A)$.

Correcting for the mass dependence of the single-particle states the binding-energy-corrected angle- and energy-integrated cross sections for one-particle transfer reactions are then given by

$$\sigma(Q_{gg}) = S_p(A) S_T(A) N \left[1 + \mathrm{erf} \left[\frac{Q_{gg} - Q_{\mathrm{opt}}}{W} \right] \right] , \tag{7}$$

with the parameters $N = 1.73 \times 10^4$, $W = 5.8$ MeV, and $Q_{\mathrm{opt}} = 0$.

The cross sections for a variety of one-neutron transfer reactions calculated from Eq. (7) are summarized in Table III. Also included are the cross sections measured for the systems ^{208}Pb+^{86}Kr (Ref. 4), ^{208}Pb+^{152}Sm, and ^{206}Pb+^{232}Th (Ref. 30). In general, the agreement between experiment and model prediction is better than 20%. Exceptions in this list involve the lightest projectile ^{12}C, where because of the small number of states involved, the applicability of this macroscopic model is questionable. The reason for the disagreement in the system ^{208}Pb+^{152}Sm, where the neutron-transfer cross sections were obtained using γ-ray techniques, is not understood.

The good agreement between experimental and theoretical cross sections obtained for many systems indicates that Q matching, binding energy of the transferred nucleons, and phase space are the dominant factors governing the one-neutron transfer cross sections. Nuclear structure effects, however, are completely neglected and might explain the discrepancies found in some cases. With this caveat in mind Eq. (7) appears to be quite reli-

TABLE III. Energy- and angle-integrated cross sections for one-neutron transfer reactions induced by various projectiles on ^{208}Pb targets.

Reaction	E_{lab} (MeV)	Q_{gg} (MeV)	σ_{exp} (mb)	σ [Eq. (7)] (mb)	Ref.
(^{12}C,^{13}C)	97.9	−2.422	22	101	11
(^{16}O,^{17}O)	104	−3.227	100	106	12
(^{28}Si,^{27}Si)	225	−13.240	<0.5	0.2	8
(^{28}Si,^{29}Si)	225	1.105	214	174	8
(^{37}Cl,^{38}Cl)	250	−1.259	160	169	7
(^{37}Cl,^{36}Cl)	250	−6.374	38	30	7
(^{46}Ti,^{47}Ti)	297	1.506	210	205	9
(^{46}Ti,^{45}Ti)	297	−9.259	7	5	9
(^{48}Ti,^{49}Ti)	300	−0.775	225	204	9
(^{48}Ti,^{47}Ti)	300	−7.690	17	15	9
(^{50}Ti,^{51}Ti)	303	−0.992	205	191	9
(^{50}Ti,^{49}Ti)	303	−7.010	28	23	9
(^{58}Ni,^{59}Ni)	375	1.631	265	225	7
(^{58}Ni,^{57}Ni)	375	−8.265	11	11	7
(^{64}Ni,^{65}Ni)	380	−1.273	160	208	This work
(^{64}Ni,^{63}Ni)	380	−5.722	60	54	This work
(^{80}Se,^{81}Se)	525	−0.667	194	216	This work
(^{86}Kr,^{87}Kr)	695	−1.858	200	200	10
(^{152}Sm,^{153}Sm)	1311	−1.502	80	218	30
(^{152}Sm,^{151}Sm)	1311	−4.330	43	121	30
(^{232}Th,^{231}Th)	1314	0.307	370	367	30

able for predicting the gross properties of one-nucleon transfer reactions.

B. Two-neutron transfer reactions

For one-neutron transfer reactions DWBA calculations, with spectroscopic factors obtained from light-ion data, can be used to obtain reasonable estimates of the transfer cross sections. Similar calculations for the two-neutron transfer reactions, however, fail by several orders of magnitude, particularly at bombarding energies close to the Coulomb barrier.[10] A macroscopic model, similar to the one mentioned above, would be very helpful for predicting the cross sections for such reactions.

The cross sections for two-neutron transfer cross sections measured with various projectiles on ^{208}Pb targets are summarized in Table IV. They are also shown in Fig. 11 as a function of the ground-state Q value together with the results obtained for other targets (see Refs. 1, 3, 14, and 32). When compared to the data for one-neutron transfer, these cross sections seem to saturate at $\sigma \approx 50$ mb for large values of Q_{gg}. This behavior can be understood from Fig. 9, since for large positive ground-state Q values one always integrates over the whole Q window. In absolute terms the cross section for a two-neutron transfer is, for the same Q_{gg} value, smaller than the corresponding value of the one-neutron transfer by about a factor of 4–5.

Similar to the one-neutron transfer reactions a binding-energy correction should be made for the two-neutron case. Since multiparticle transfer reactions at low bombarding energies have been found to proceed dominately via multistep processes, the average binding energy for each of the two transfer steps was used for calculating B_i and B_f in Eq. (5). These binding-energy-corrected cross sections are shown in Fig. 12 together with data involving other target nuclei. Also included in Fig. 12 are the reduced cross sections for one-neutron transfers and one case for a three-neutron transfer reaction ^{208}Pb(^{48}Ti,^{51}Ti)^{205}Pb (Ref. 3) where a full angular distribution for this process has been measured. The solid lines are the result of Eq. (6) fitted to the case for the one-neutron transfer reactions and scaled down by factors of about 4 or 16 for the two- and the three-neutron transfer reaction, respectively. The overall agreement of the solid lines with the data is quite good.

Two observations can be made from Fig. 12. Each step

TABLE IV. Energy- and angle-integrated cross sections for two-neutron transfer reactions induced by various projectiles on ^{208}Pb targets.

Reaction	E_{lab} (MeV)	Q_{gg} (MeV)	σ_{exp} (mb)	Ref.
(^{28}Si,^{30}Si)	225	4.974	60	8
(^{30}Si,^{32}Si)	225	1.694	40	8
(^{37}Cl,^{39}Cl)	250	0.074	38	7
(^{46}Ti,^{48}Ti)	297	6.394	52	9
(^{48}Ti,^{50}Ti)	300	4.982	54	9
(^{50}Ti,^{52}Ti)	303	0.070	45	9
(^{58}Ni,^{60}Ni)	375	6.278	61	7
(^{64}Ni,^{66}Ni)	380	0.985	40	This work
(^{80}Se,^{82}Se)	525	1.864	47	This work
(^{232}Th,^{230}Th)	1314	2.547	98	30

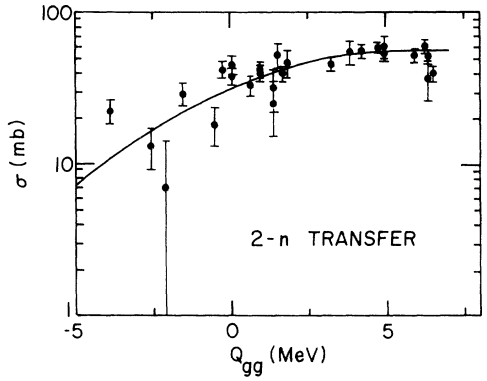

FIG. 11. Energy- and angle-intergrated two-neutron transfer cross sections induced by various projectiles on ^{208}Pb, Sn, and Ni targets as a function of Q_{gg}. The solid line serves to guide the eye.

in a multistep neutron-transfer reaction seems to reduce the cross section at a given Q value by about a factor of 4–5. From the data shown in Fig. 12 the same cross-section ratios between energy-integrated one- and two-neutron transfer reactions are observed for reactions involving Ni, Sm, and Pb as well as Sn nuclei, where in two-neutron transfer reactions (for distant collisions) large enhancement factors have been observed.[32]

VI. SYSTEMATICS OF CHARGED-PARTICLE TRANSFERS

A. One-proton transfer

An extension of this model to charged-particle transfers is more complicated since the optimum Q value Q_{opt} entering Eq. (7) is both system and energy dependent. Furthermore, charged-particle transfers have smaller cross sections than neutron-transfer reactions and therefore only few data involving medium-mass projectiles have been obtained so far. In Fig. 13(a) one-proton transfer cross sections are plotted as a function of the ground-state Q value Q_{gg}. All of these cross sections correspond to one-proton-stripping reactions on ^{208}Pb targets, e.g., (^{58}Ni,^{57}Co) (Ref. 33), (^{48}Ti,^{47}Sc) (Ref. 9), (^{28}Si,^{27}Al) (Ref. 8), and (^{37}Cl,^{36}S) (Ref. 31). Also included are two data points from (^{28,30}Si) induced reactions on ^{206}Pb (Ref. 34). It should be mentioned that all these proton-stripping reactions are generally well Q matched. Proton pickup reactions induced by medium-weight projectiles and populating low-lying states are mostly Q mismatched. Therefore only upper limits can be quoted.[2] It is interesting to note that the absolute strength for the one-proton-stripping reaction is comparable to the strength of the two-neutron transfer reaction. Figure 13(b) shows the same data [including the upper limit for the (^{28}Si,^{29}P) reaction from Ref. 2] plotted as a function of $Q_{gg}-Q_{opt}$, where Q_{opt} was calculated according to Ref. 20 as $Q_{opt}=E_{c.m.}[(z'Z')/zZ-1]$, where zZ and $z'Z'$ are the charges in the entrance and exit channels, respectively. The same binding-energy corrections as for neutron-transfer reactions have been applied to the data, using the binding energies of the transferred proton in projectile and residual nucleus, respectively. The solid line is the result of a least-squares fit to the data using Eq. (6). Although the data follow a similar systematics as ob-

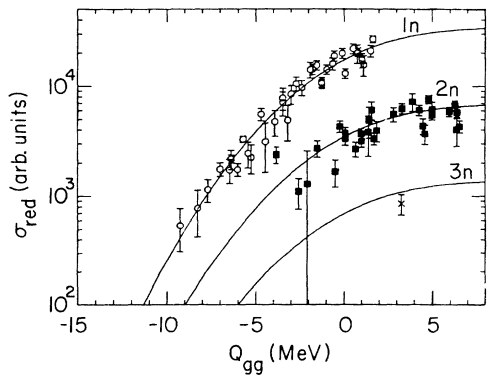

FIG. 12. Binding-energy-corrected one-, two-, and three-neutron transfer cross sections induced by various projectiles plotted as a function of the ground-state Q value Q_{gg}. The solid lines are explained in the text.

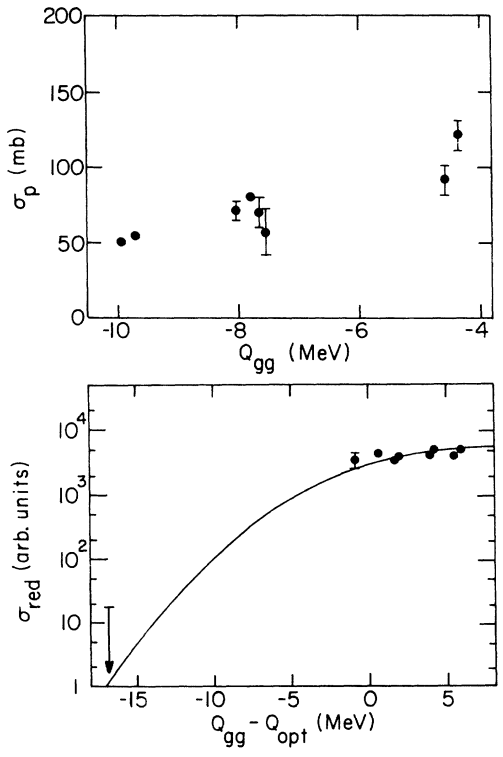

FIG. 13. (a) Angle- and energy-integrated cross sections for one-proton transfer reactions induced by various projectiles on ^{208}Pb targets, plotted as a function of the ground-state Q value Q_{gg}. (b) Binding-energy-corrected one-proton transfer cross sections plotted as a function of $Q_{gg}-Q_{opt}$. The solid line was calculated using Eq. (6). See text for details.

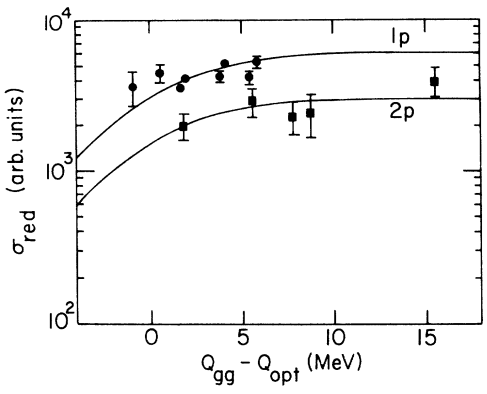

FIG. 14. Binding-energy-corrected one- (dots) and two- (squares) proton transfer cross sections plotted as a function of the $Q_{gg} - Q_{opt}$. The solid lines are explained in the text.

served for the one- and two-neutron transfer reactions, it is clear that more data points, in particular for Q-mismatched one-proton-pickup reactions, are needed.

B. Two-proton transfer

In some cases the two-proton transfer strength has been determined as well. The binding-energy-corrected cross sections from these measurements are shown as solid points in Fig. 14 together with the data from one-proton transfer reactions. They correspond to the two-proton-stripping reactions (^{30}Si,^{28}Mg) (Ref. 2), (^{37}Cl,^{35}P) (Ref. 34), (^{48}Ti,^{46}Ca) (Ref. 3), (^{58}Ni,^{56}Fe) (Ref. 33), and (^{80}Se,^{78}Ge). [The latter reaction includes also contributions from the (^{80}Se,^{78}As) reactions.] As for the one-proton transfer reactions these processes are usually well Q matched and do not show a large variation as a function of $Q_{gg} - Q_{opt}$. Compared to the neutron-transfer case, however, it is evident that the ratio between one- and two-proton transfer cross sections is only about 2 (see the two solid lines in Fig. 14) while it is about 4–5 for the corresponding neutron transfers. This difference might be caused either by a reduction of the one-proton transfer probability or by an increase of the two-proton transfer probability similar to the observation in Ref. 35. A comparison of one-proton-stripping reactions induced by ^{28}Si ions on ^{40}Ca, ^{48}Ca, and ^{208}Pb with DWBA predictions (Refs. 2, 36, and 37) has shown that in all cases where spectroscopic factors are known the one-proton-stripping strength is well accounted for.

VII. SUMMARY

Transfer cross sections for the systems ^{64}Ni and ^{80}Se+^{208}Pb have been measured with good mass resolution at 380 and 525 MeV bombarding energy, respectively. Similar to the observations from other systems the quasielastic cross sections are dominated by the one-neutron transfer reactions (^{64}Ni,^{65}Ni) and (^{80}Se,^{81}Se). In contrast to lighter systems, however, deep-inelastic reactions are becoming more important for these heavier systems. The energy- and angle-integrated one-neutron transfer cross sections are found to follow a simple systematic trend which is based on Q matching and includes corrections for binding-energy and phase-space (single-particle level-density) effects. Two-neutron transfer cross sections also follow the same behavior but with a strength which is smaller than the one-neutron strength by a factor of about 4–5. These systematics can provide estimates for energy- and angle-integrated neutron-transfer cross sections for other systems. The systematics has been found to work with projectiles in the mass range $A = 16$–80 and with target nuclei between 60 and 232. The few data available so far involving proton-transfer reactions indicate that this semiclassical description is applicable for charged-particle transfer reactions as well. A comparison of the ratios between one- and two-particle transfer cross sections indicates that the two-proton transfer reaction is somewhat enhanced relative to the two-neutron case.

This work was supported by the U.S. Department of Energy, Nuclear Physics Division, under Contract W-31-109-ENG-38.

*Present address: CRN Strasbourg, F-67037 Strasbourg, France.
†Present address: KVI Groningen, The Netherlands.
‡Present address: SUNY, Stony Brook, NY 11794.
§Present address: Department of Physics, Tsinghua University, Beijing, People's Republic of China.
**Present address: Lawrence Livermore Laboratory, Livermore, CA 94550.

[1]K. E. Rehm, D. G. Kovar, W. Kutschera, M. Paul, G. S. G. Stephans, and J. L. Yntema, Phys. Rev. Lett. **51**, 1426 (1983).
[2]J. J. Kolata, K. E. Rehm, D. G. Kovar, G. S. F. Stephans, G. Rosner, and H. Ikezoe, Phys. Rev. C **30**, 125 (1986).
[3]K. E. Rehm, A. M. van den Berg, J. J. Kolata, D. G. Kovar, W. Kutschera, G. Rosner, G. S. F. Stephans, and J. L. Yntema, Phys. Rev. C **37**, 2629 (1988).
[4]A. H. Baltz, P. D. Bond, O. Hansen, J. Cheng-Lie, P. R. Christensen, S. Pontoppidan, F. Videbaek, D. Schüll, S. Wen-Quing, and H. Freiesleben, Phys. Rev. C **29**, 2392 (1986).
[5]S. Steadman and M. J. Rhoades-Brown, Annu. Rev. Nucl. Sci. **36**, 649 (1986).
[6]M. Beckerman, Rep. Prog. Phys. **51**, 1047 (1988).
[7]See, for example, H. Esbensen, Nucl. Phys. **A352**, 147 (1981); C. H. Dasso, S. Landowne, and A. Winther, *ibid.* **A405**, 381 (1983); P. Jacobs and U. Smilansky, Phys. Lett. **127B**, 313 (1983); S. Landowne and S. C. Pieper, Phys. Rev. C **29**, 1352 (1984); M. J. Rhoades-Brown and P. Braun-Munzinger, Phys. Lett. **136B**, 19 (1986).
[8]K. E. Rehm, F. L. H. Wolfs, A. M. van den Berg, and W. Henning, Phys. Rev. Lett. **55**, 280 (1985).
[9]S. Landowne and A. Vitturi, in *Treatise on Heavy Ion Science,*

edited by D. A. Bromley (Plenum, New York, 1985), Vol. 1.
[10]R. J. Asciutto and E. A. Seglie, in *Treatise on Heavy Ion Science,* edited by D. A. Bromley (Plenum, New York, 1985), Vol. 1.
[11]K. S. Toth, J. L. C. Ford, Jr., G. R. Satchler, E. E. Gross, D. C. Hensley, S. T. Thornton, and T. C. Schweizer, Phys. Rev. C **14**, 1671 (1976).
[12]S. C. Pieper, M. H. Macfarlane, D. H. Gloeckner, D. G. Kovar, F. D. Bechetti, B. G. Harvey, D. L. Hendrie, H. Homeyer, J. Mahoney, F. Pühlhofer, W. von Oertzen, and M. S. Zisman, Phys. Rev. C **18**, 180 (1978).
[13]J. R. Erskine, T. H. Braid, and J. G. Stoltzfus, Nucl. Instrum. Methods **135**, 67 (1976).
[14]A. M. van den Berg, W. Henning, L. L. Lee, K. T. Lesko, K. E. Rehm, J. P. Schiffer, G. S. F. Stephans, and F. L. H. Wolfs, Phys. Rev. C **37**, 178 (1988).
[15]M. H. Macfarlane and S. C. Pieper, Argonne National Laboratory Report No. ANL-76-11 (Rev. 1), 1978 (unpublished).
[16]M. L. Halbert, Nucl. Data Sheets **28**, 179 (1979).
[17]J. Barrette, M. Barrette, G. Lamoureux, S. Monaro, and S. Markiza, Nucl. Phys. **A235**, 154 (1974).
[18]M. J. Martin, Nucl. Data Sheets **47**, 797 (1986).
[19]A. J. Baltz, Phys. Rev. C **25**, 240 (1982).
[20]P. J. A. Buttle and L. J. B. Goldfarb, Nucl. Phys. **A176**, 299 (1971).
[21]H. J. Körner, G. E. Rathke, C. N. Davids, D. G. Kovar, W. Kutschera, K. E. Rehm, and F. L. H. Wolfs (unpublished).
[22]R. Bock, Y. T. Chu, M. Dakowski, A. Gobbi, E. Grosse, H. Olmi, H. Sann, D. Schwalm, U. Lynen, W. Müller, S. Bjørnholm, H. Esbensen, W. Wölfli, and E. Morenzi, Nucl. Phys. **A388**, 334 (1982); B. Back, private communication; W. Q. Shen, J. Albinski, A. Gobbi, S. Gralla, K. D. Hildenbrand, N. Herrmann, J. Kuzminski, W. F. J. Müller, H. Stelzer, J. Toke, B. B. Back, S. Bjørnholm, and S. P. Sørensen, Phys. Rev. C **36**, 115 (1987).
[23]F. Videbaek, R. B. Goldstein, L. Grodzins, S. G. Steadman, T. A. Belote, and J. D. Garrett, Phys. Rev. C **15**, 954 (1977).
[24]F. L. H. Wolfs, W. Henning, K. E. Rehm, and J. P. Schiffer, Phys. Lett. **196**, 113 (1987).
[25]W. E. Frahn, Nucl. Phys. **A302**, 281 (1978).
[26]J. C. Acquadro, M. S. Hussein, D. Pereira, and O. Sala, Phys. Lett. **100B**, 321 (1981).
[27]U. Brosa and W. Westmeier, Nucl. Phys. **A441**, 109 (1985).
[28]M. Beckerman, R. L. Auble, F. E. Bertrand, J. L. Blankenship, B. L. Burks, C. W. Glover, R. O. Sayer, G. R. Satchler, D. Shapira, and R. L. Varner, Phys. Rev. Lett. **58**, 455 (1987).
[29]A. M. van den Berg, K. E. Rehm, D. G. Kovar, W. Kutschera, and G. S. F. Stephans, Phys. Lett. B **194**, 334 (1987).
[30]F. W. N. de Boer, H. J. Wollersheim, H. Emling, H. Grien, E. Grosse, W. Spreng, G. Eckert, Th. W. Elze, K. Stelzer, and Ch. Lauterbach, Z. Phys. A **325**, 457 (1986).
[31]K. E. Rehm *et al.* (unpublished).
[32]W. von Oertzen, B. Gebauer, H. G. Bohlen, F. Busch, and D. Schüll, Z. Phys. A **313**, 189 (1983).
[33]F. L. H. Wolfs *et al.* (unpublished).
[34]R. Vojtech, Ph. D. thesis, University of Notre Dame, 1988 (unpublished).
[35]R. Künkel, W. von Oertzen, B. Gebauer, H. G. Bohlen, H. A. Bösser, B. Kohlmeyer, F. Pühlhofer, and D. Schüll, Phys. Lett. B **208**, 355 (1988).
[36]S. D. Hoath, G. C. Morrison, J. M. Nelson, F. Videbaek, P. D. Bond, O. Hansen, M. J. Levine, C. E. Thorn, and W. Trautmann, Phys. Lett. **154B**, 33 (1985).
[37]M. F. Vineyard, D. G. Kovar, G. S. F. Stephans, K. E. Rehm, G. Rosner, H. Ikezoe, J. J. Kolata, and R. Voijech, Phys. Rev. C **33**, 1325 (1986).